DOE/PC/79678--T3

DOE/PC/79678--T3

DE90 003900

SEMI-ANNUAL REPORT

for

AN INNOVATIVE DEMONSTRATION OF HIGH POWER DENSITY IN A COMPACT MHD GENERATOR

CONTRACT NO. DE-AC22-87PC79678

SUBMITTED TO:

UNITED STATES DEPARTMENT OF ENERGY
PITTSBURGH ENERGY TECHNOLOGY CENTER
P.O. BOX 10940
PITTSBURGH, PA 15236-0940

PREPARED BY:

H. J. SCHMIDT
J. T. LINEBERRY

SUBMITTED BY:

THE UNIVERSITY OF TENNESSEE SPACE INSTITUTE
TULLAHOMA, TENNESSEE 37388-8897
(615) 455-0631

SEPTEMBER 1988

Abstract

The University of Tennessee Space Institute is conducting a two year program to demonstrate high power density operation of a combustion driven magnetohydrodynamic generator. To achieve high power density an energetic fuel comprised of powdered aluminum and carbon fuel will be burnt with gaseous oxygen in a hybrid combustion scheme for which there is no precedent experimental data base.

This semi-annual report summarizes the experimental design and discusses the trade-offs and technical risks involved which are more fully described in the previous first semi-annual report. During the period covered by the present report, April - September 1988, detail design of the combustor system was completed and a fabrication subcontract awarded to REDEVCO, Inc. of West Valley, UT. A high pressure oxidizer system was also designed and procurement initiated for its components. The latter was necessitated when the detailed design calculations indicated that to achieve the experimental goals, combustion pressures well in excess of available gaseous oxygen systems were required. As discussed, a simple bottle storage system will be used.

TABLE OF CONTENTS

1.0 INTRODUCTION

Magnetohydrodynamic (MHD) energy conversion is a candidate technology for satisfying pulse power requirement for advanced weapon and discrimination systems for the Strategic Defense Initiative. However, to be competitive with alternative pulse power systems the characteristic power per unit weight and volume requires performance improvement beyond that demonstrated to date.

The present program being conducted by the University of Tennessee Space Institute (UTSI) is a high risk experimental program to demonstrate that high power density operation of a combustion driven MHD generator is feasible. To achieve high power density and implied commensurate low system volume and weight densities, it is necessary to use an energetic fuel. In the present program, a solid fuel comprised of a powdered aluminum-carbon mixture seeded with potassium carbonate is to be burned with gaseous oxygen. Theoretical calculations indicate that the resulting combustion plasma has an electrical conductivity sufficiently high to result in power density levels of several hundred megawatts per cubic meter. However, there is little knowledge in general or experience in particular in the practical aspects of burning this fuel in the hybrid combustor scheme and this is a high risk area. The risk is balanced by the use of minimal cost flow train components of heat sinking design. A subordinate element of the program is to demonstrate that minimal cost "throw away" components are a viable alternative to the more expensive but repairable designs employing active cooling as commonly used in more conventional experimental investigations.

The program is a two-year effort with the first year being devoted to the overall test design in general. The detail design, procurement and testing of the combustor alone is the primary effort focus in the first year. During the second year, two generator channels will be built and tested with the combustor for the power density demonstration. While the first year was involved

primarily with the combustor, the combustor design and fuel selection are intimately connected with the channel lofting. Therefore, considerable effort in the study of the overall system was expended although the detailed mechanical design of the generators is deferred to the second year.

The present report reviews the first year's effort. This review includes the fuel selection, operating point specification, channel lofting, combustor design as well as the oxidizer system and facility preparation for initial combustor testing. The combustor is currently being fabricated by REDEVCO with delivery expected in early November 1988. The program schedule has slipped. However, it is anticipated that the combustor testing will commence in December 1988 and be completed by February 1989 which should not significantly delay the program completion date.

2.0 FUEL SELECTION

The power density in an MHD generator is the electrical power output per unit of internal volume of the generator. As such, it is a fundamental parameter which governs the aggregate MHD system size and weight for a given power output level. The maximization of the power density, which is the goal of the present effort, is therefore a first step in the evolution of compact high power MHD power systems.

To a first order, the power density in an MHD generator is proportional to the product of the plasma conductivity with the squares of the plasma velocity and imposed magnetic field strength. That is

$$\text{power density} \sim \frac{\sigma u^2 B^2}{4} \tag{1}$$

where σ is the conductivity, u is the plasma velocity and B is the field strength. In this proportionality, it is convenient to further subdivide the expression into the terms B^2 and the product $\frac{\sigma u^2}{4}$ where the latter is termed the power density parameter. The power density parameter, which can also be thought of as the power density for a field of 1 Tesla, is a plasma characteristic. In general, not only does it vary with the chemical composition of the plasma but also with the thermodynamic state of a given composition. In particular, the power density parameter is a function of the plasma temperature and exhibits an optimal value. The plasma conductivity is an increasing function with temperature while plasma velocity is a decreasing function with temperature. The fuel selection for high power density involves two considerations. First, the fuel must be energetic to produce high temperatures and plasma conductivity; and second, when expanded from the combustor state, the plasma should maintain a high value of the power density parameter.

In the present system an aluminum-carbon mixture burned with gaseous oxygen has been selected as the plasma source. Aluminum has an extremely high heat of combustion (14,150 BTU/lbm) when burned with oxygen. However, the resulting aluminum oxides will be in condensed phases at the pressures and temperatures of interest and will not significantly contribute to the plasma collision processes upon which the plasma conductivity and MHD interaction are based. The carbon portion of the fuel will yield gaseous species CO and CO_2 which will comprise the major volumetric components of the plasma. The plasma is seeded with potassium carbonate to provide high conductivity resulting from the ionization of the potassium. The absence of hydrogen in the plasma products is also conducive to high plasma conductivity since water has a high collision cross-section and the negative hydroxyl ion can deplete free electrons from the plasma.

While attractive from theoretical considerations, there is little known experimental data or practical experience in using this fuel combination. The only known application of the aluminum-carbon-oxygen plasma generation system in a high performance MHD system has been in the Soviet Union[1,2]. The Soviet investigators used a conventional combustor in which the seeded aluminum-carbon fuel was injected as a powder. For the present work, a hybrid combustion system in which fuel is cast in a grain within the combustor will be used. Such a system has many of the simplicities of a solid propellant rocket engine. However, by introducing the oxidizer separately, gaseous oxygen in this case, the ability to stop and restart is possible and as such this system is inherently safe and simple. In addtion, the fuel grain also serves as a thermal shield as it is consumed allowing for a simple thermal control system.

2.1 Combustion Characteristics

Calculations have been performed to assess the suitability of the selected fuel for the MHD applications. These calculations considered: relative

aluminum to carbon content, seed weight percentage and type, combustor pressure, stoichiometry, and binder content. Results and discussions of these calculations are fully described in the semi-annual report[3] and for brevity will not be repeated here. In summary, the calculations showed that plasma conductivity increases with increasing aluminum content, equivalence ratio, and seed rate while it decreases with increasing combustor pressure. The calculations also showed that binder content, which can be up to 20% of the fuel composition by weight, must also be taken into account.

With regard to the seed material, cesium by virtue of its lower ionization potential would result in higher plasma conductivity than potassium. Figure 1 presents calculated plasma conductivity at the combustor conditions for potassium and cesium carbonate seed materials for various weight percentages of seeding. As indicated in the figure, higher conductivity levels are indicated with the cesium. On the weight basis, the conductivity maximizes for 12% and 5% for the cesium and potassium respectively. However, note that since the molecular weight of the cesium carbonate is 2.35 times that of potassium carbonate the maximum conductivity occurs at approximately the same molar fraction. Cesium is considerably more expensive than potassium partially due to its lower abundance in nature. Therefore, potassium was selected for the present investigation as it would be the more practical choice in a widespread use. Clearly cesium would be of utility is maximizing conductivity, and it may be beneficial to do so in extension to the present or similar program. For example, in the present program a 3.2 Tesla magnet will be used. From the previous discussion, the power density will vary as the product of the conductivity and the square of the field strength. Thus, as a crude estimate one could expect the power density with a 14% cesium seed percentage of a 3.2T field to be equivalent to that of a 5% potassium seed level with a 3.7T field. In a practical device it again may be more beneficial

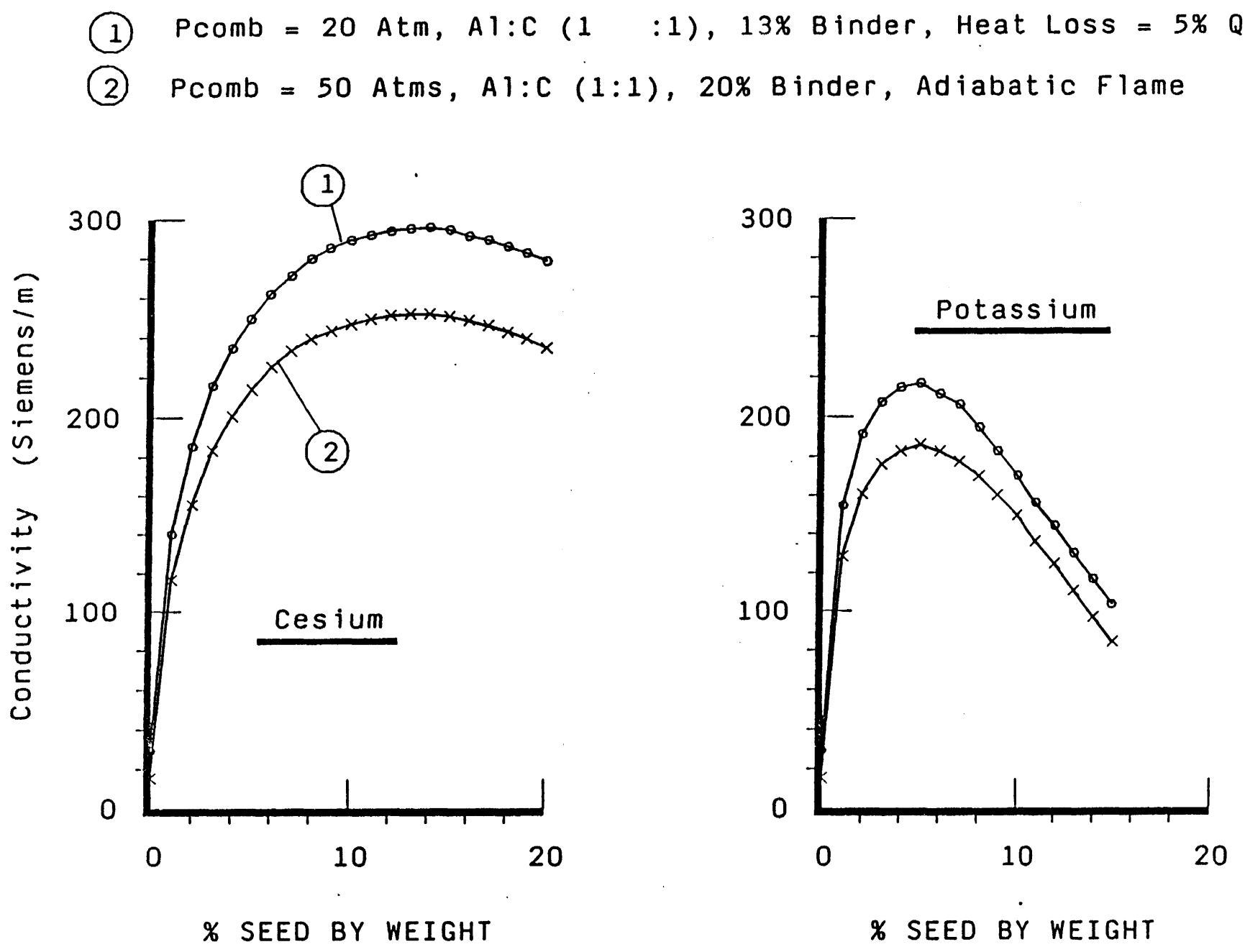

Figure 1. Plasma Conductivity Variation with Seeding Percentage Potassium and Cesium at Variable Combustion Conditions.

to increase the field rather than the striving for the maximum conductivity. The point is, that by using a highly energetic fuel, sufficient conductivity results for a practical application with the more available and cheaper potassium seed. The present investigation should therefore not be looked on as a maximum effort to achieve a high power density by maximizing the plasma conductivity. Rather, it should be more appropriately viewed as using a "low quality" seed with an energetic fuel as contrasted with using a "high quality" seed with a less energetic fuel. On the basis of the calculated results, a nominal fuel composition has been selected as a 50% mixture by weight of aluminum with carbon, with up to 20% by weight epoxy binder and seeded with 5% by weight potassium carbonate. The desired stoichiometry of combustion is 0.77 (equivalence ratio = 1.30).

2.2 Power Density

As previously pointed out the conductivity in the combustor while serving as a figure of merit is subordinated to the power density parameter in the generator. The potential to produce electrical power in the expanded plasma states is of primary importance. During the expansion, the plasma temperature and pressure drop while its velocity increases. While the plasma conductivity increases with decreasing pressure at constant temperature, the temperature dependence is strong and dominate so that the conductivity in general decreases as the plasma expands.

The evolution of the power density parameter during the expansion process through the nozzle can conveniently be described on a nomograph as depicted in figure 2. The figure is actually a nozzle design nomograph and contains a considerable condensation of information which requires detailed explanation. The figure is a depiction of nozzle expansion processes for a predetermined and constant nozzle exit area (i.e. generator entrance area) and variable throat area. For the present experimental system, the dimensional constraints

MHD GENERATOR ENTRANCE MAP

Combustion of Al:C (1:1) with Binder, K_2CO_3 (5% K) in Gaseous O_2

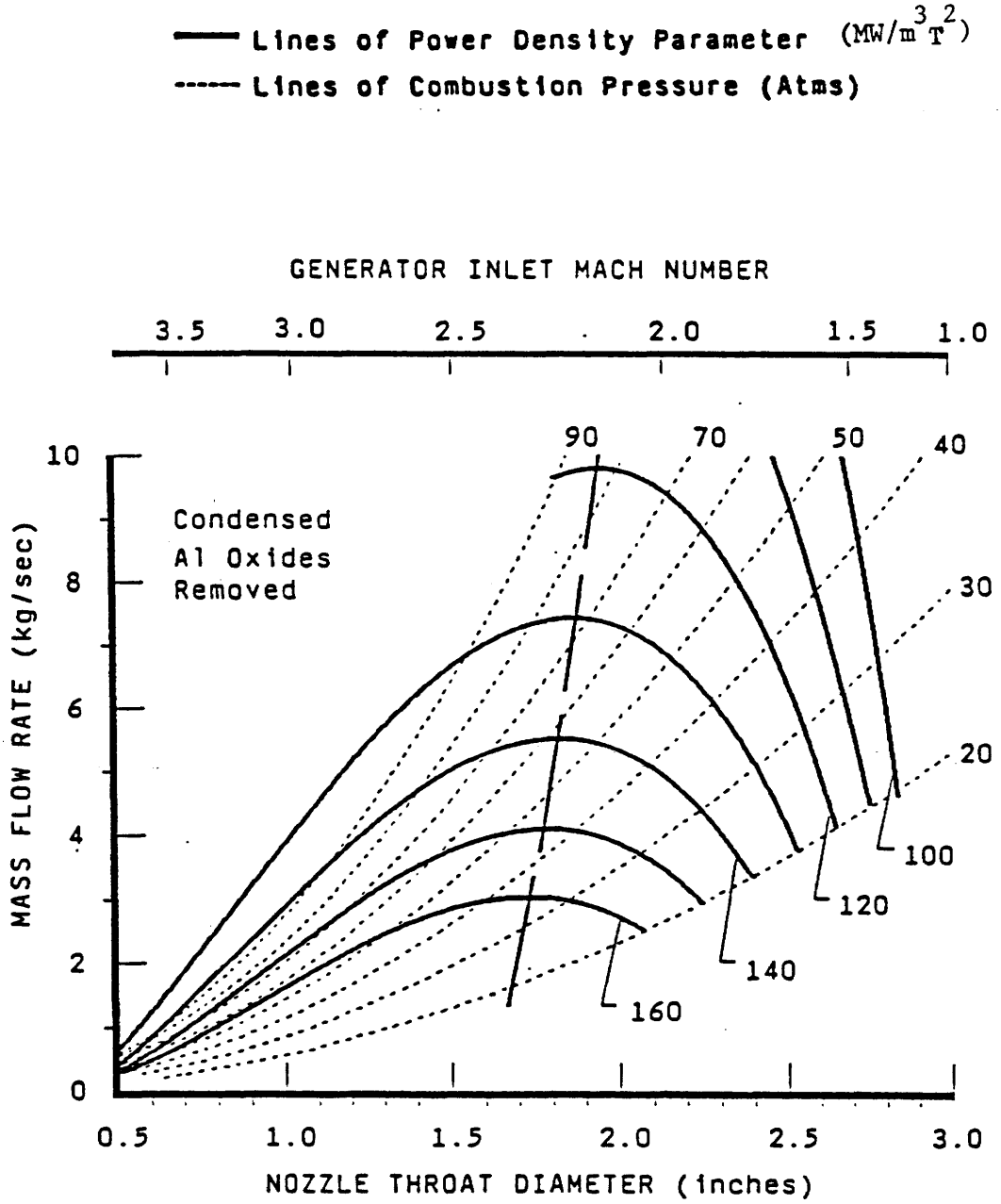

Figure 2. Nozzle Design Nomogram for a Three (3) Inch Diameter Exit Based on Calculations with Condensed Species Removed.

of an existing magnet bore effectively imposes a constraint on the maximum internal diameter of a generator which is three (3) inches. Figure 2 is therefore, based on a fixed nozzle exit area diameter of three (3) inches. Consider first, the dotted lines in figure 2. These are combustion pressure isolines which provide a graphical solution for the mass flow rate (ordinate) as a function of the nozzle throat diameter (abscissa). Thus, for a given throat size the mass flow rate as a function of combustor pressure is readily determined. Conversely for a constant mass flow rate the functional relation between the combustion pressure and throat size is similarly depicted.

Since the plot is based on a fixed nozzle exit area, the variable throat implies a variable area ratio or equivalently an expansion to a variable flow Mach number at the nozzle exit. The resulting exit Mach number is given by the scale at the top of the figure. Thus, when the throat diameter is three (3) inches (the same as the exit diameter) the flow Mach number is one (1), and as the throat diameter diminishes the exit Mach number (and area ratio) increases accordingly. The Mach number relation depends on the plasma specific heat ratio which may have a slight pressure dependence during expansion as a consequence of thermochemical species variations. The Mach number scale is correct for a combustion pressure of 50 atm. but will be approximately correct for all other cases depicted.

Figure 2 presents not only the mass flow relation for the nozzle but by virtue of the fixed exit area, also infers an exit thermodynamic state for each combination of throat size, mass flow, and combustion pressure. Since the power density parameter is derivable from the plasma state variables, it can also be plotted on the figure. The solid lines in figure 2 are isolines of the power density parameter and as indicated they are convex downward and exhibit peak or optimal values. As an illustration, consider a hypothetical case of a constant mass flow of 4 kg/sec. In figure 2, the power density

parameter value of 140 results at a combustor pressure of 90 atm with a 1.2 inch diameter throat and at a pressure of 25 atm with a 2.3 inch diameter throat. The maximum value of 150 MW/m^3 occurs at a pressure of approximately 45 atm, and a throat diameter of approximately 1.75 inches which is the peak of the 150 MW/m^3 power density parameter isoline. This illustrates the optimization of the expansion process with regard to the power density. The optimal points lie on the peaks of the power density isolines, and the locus of these peaks is superimposed as a broken line in figure 2. To the left of the optimal line the velocity squared term increases faster than the conductivity decreases as the maximum power density value is approached. The converse behavior occurs to the right of the optimal line. From this figure, it can be concluded as a generality that irrespective of the mass flow or combustion pressure, an optimal generator entrance Mach number should be in the range 2.25 to 2.5 for this fuel combination.

In addition, one can also infer the effects of expected nozzle throat erosion from the figure. Under the assumption that the fuel surface recession rate is independent of combustion pressure, the mass flow will remain constant. However, erosion at the nozzle throat will increase its effective diameter and result in a lowering of the combustor pressure. If the initial design point for the nozzle is to the left of the locus of peak values, the power density should increase as the throat enlarges or if it were at or to the right of the optimal, the power density should decrease as the throat enlarges.

Figure 2 is not a universal nomogram in that it is predicated on a particular combustion system of a particular seeding rate subject to ideal computational assumptions. First, let us consider the conductivity model. Figure 2 is based on a 5% by weight potassium seed. Other seed percentages or cesium could be expected to change the plasma conductivity. As a crude estimate, such a perturbation can be taken to be uniform in that the values of

power density parameter would change, but the form of the relations depicted in figure 2 would not drastically change. The conductivity of plasma containing aluminum species itself is not well understood. At high pressure and high temperatures significant fractions of AlO_2^- and AlO^- ions which deplete the free election concentration can be present. A proper accounting for these effects is uncertain, particularly in the case of the AlO^- ion. Crawford and Lineberry[4] have indicated that up to a 50% reduction in conductivity can result by inclusion of this ion in comparison to its neglection in Al:C combustion schemes. The widely used JANAF tables for electrophysical property data of chemical species are inconsistent with regard to AlO^-. All calculations performed in support of the present effort have not considered any possible effect of the AlO^- species on the electrical transport properties of the plasma.

A second important aspect of the Al:C fuel is the treatment of the aluminum oxides in the expansion and MHD processes. The principal oxide Al_2O_3 will be in a condensed state at the pressures and temperatures of interest in the nozzle and generator. The calculations are based on the NASA 273 thermochemical equilibrium code. In equilibrium calculations, the underlying assumption is that the latent heat of condensation is available to the gaseous species present during the expansion process. In the present case where residence times are short, this may not be valid. The results presented in figure 2 have been "doctored" in that condensed species have been eliminated from the expansion. That is, the combustor flame temperature was calculated with all species present. Only the gaseous species, however, were considered during the expansion process.

In contrast, the nozzle design nomogram for calculations including the condensed species is given in figure 3 for the same fuel composition as in figure 2. In comparing the figures, the inclusion of the condensed species

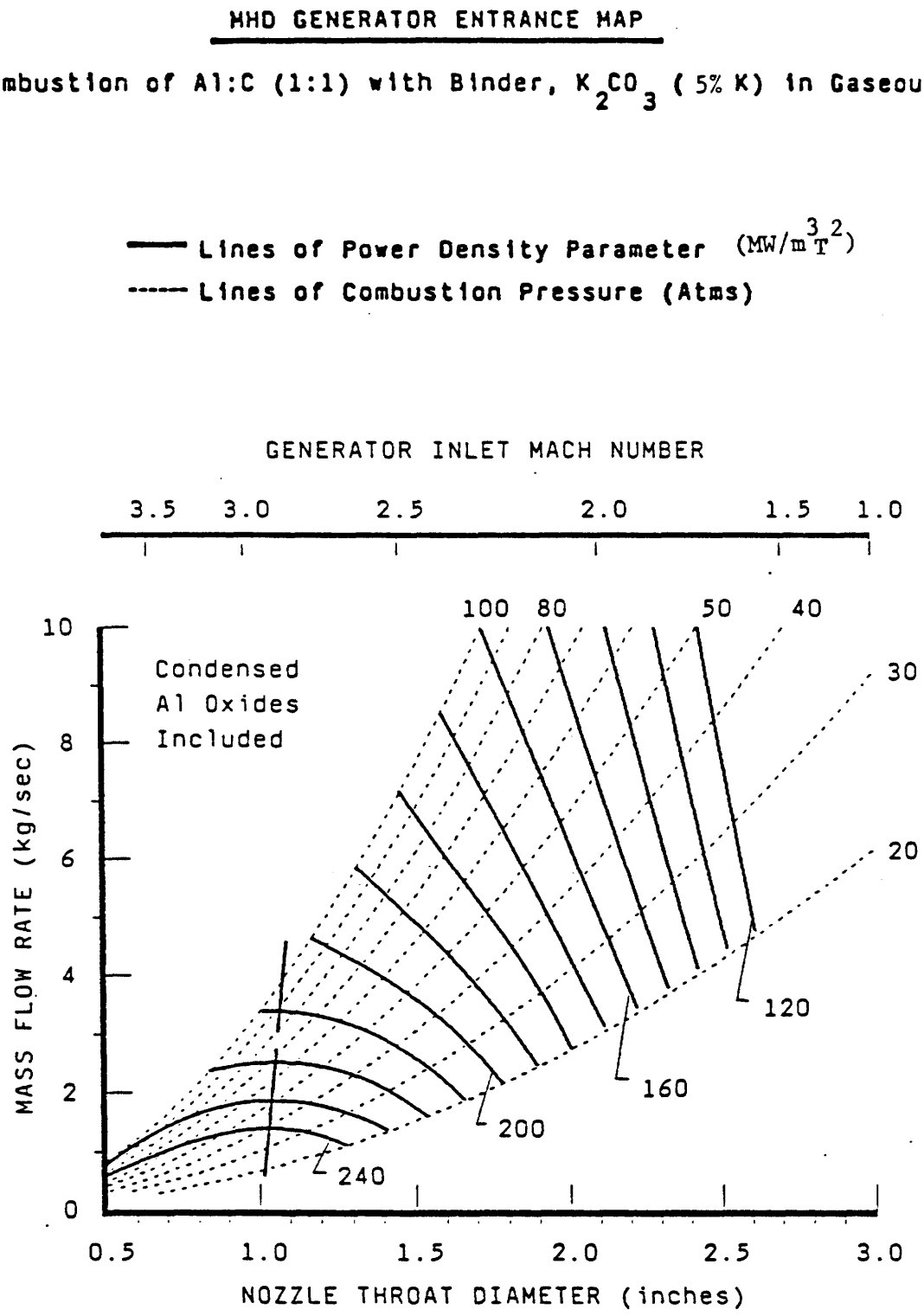

Figure 3. Nozzle Design Nomogram for a Three (3) Inch Diameter Exit Based on Calculations with All Species Considered.

results in markedly increased values for the power density parameter. The two figures represent extremes insofar as the modeling is concerned, and figure 2 is the more conservative case upon which the design calculations should more appropriately be based.

3.0 DESIGN STUDIES

While the first year of the present program was concerned primarily with the combustor development and checkout, it was necessary to consider the experimental flow train in its entirety. To balance the costs and risks in the effort, an existing 3.2 Tesla magnet will be used for the powered testing. The MHD process is a volumetric process. That is, while the various loss mechanisms: viscous effects, thermal losses, electrode voltage drops, etc. scale with internal wetted area, the power scales with volume. As a consequence, it is desirable to conduct the experiment with a generator channel whose internal cross-sectional area is as large as can be accommodated by the magnet bore yet satisfies the program criteria. In this section, the design criteria and constraints are discussed in further detail along with mechanical design of the combustor and nozzle. As part of the design studies, the lofting and performance of the generator channel was completed and is discussed. The mechanical design of the generator channels, as well as their construction and testing, however, are to be addressed in the second year's program effort.

3.1 Design Criteria

The present program is guided by several criteria which are sought to be satisfied during all phases from conceptual design through testing. In summary, these criteria are:

Maximize MHD power density,
Minimize combustion pressure,
Maintain simplified mechanical design,
Maximize system integrity/reliability
Minimize fabrication and operating costs,
and, Maximize to the extent possible the utilization of existing equipment.

The first item is a statement of the program objective. Note, that it does not imply power maximization, but rather power per unit volume. In keeping with this objective, emphasis is placed in achieving high power in a

small generator with little regard being paid to optimizing the generator for total power or fullness of utilization of the available magnetic field. The minimization of combustion pressure is desirable from safety and operational aspects as well. As shown previously in figure 2, lower combustor pressures favor higher potential power densities. This is somewhat misleading, however. For the high interaction expected in the experiments one must have sufficient pressure available to drive the plasma against the magnetic field, and as will be shown later in section 3.4, low pressures are not a viable alternative for a workable size generator. Similarly, to maximize power production from a given magnetic field one would design the generator channel to utilize the full available pressure drop across the entirety of the available magnetic field. In such an instance pressure recovery in a diffuser downstream of the channel becomes an extremely important factor. Again, this concern is not deemed important as the present testing is not solely concerned with total power produced or as more commonly referenced, the enthalpy extraction. The rate of power production or rate of enthalpy extraction per unit volume is the primary goal.

The remaining four items in the above list of criteria are all related to minimizing the cost. To meet these criteria the conceptual design of a hybrid combustor and a heat sinked flow train has been developed. The hybrid combustor is comprised of a fuel grain cast within the combustor with a gaseous oxygen oxidizer supplied externally to the combustor. Advantages of the design are its inherent simplicity, in that no fuel metering or control is necessary, it is stoppable and restartable, and the fuel grain itself serves as a thermal shield. Disadvantages are that run time is limited and with no known prior experience with this fuel in this type of combustion system, risks are involved. The burning characteristics are unknown, even its physical characteristics, such as its cast density and the relation of casting density

to burning rate are only estimable at the present. In fact, the testing of the combustor will provide information on some of the unknown fuel characteristics which will be employed in the generator design and testing phases in the following year. Simplicity of the design has been of high priority and some of the features adopted to maintain simplicity are:

- A reusable combustor which can be repacked with fuel for multiple firings.
- A nozzle designed with an outer structural shell and interchangeable, variable internal graphite inserts for multiple testing and variable operation.
- Two-terminal generator configurations to minimize the complexity of the electrical network.
- Utilize graphite material for plasma exposed internal surfaces (electrodes and nozzle) to provide heat sinking and ablative shielding.
- Simple internal flow lofting, i.e., a circular flow cross-section and straight internal. walls.
- Use of a common diffuser and downstream quench system with disregard to optimization of diffuser performance.
- Minimization of instrumentation, i.e., measurement of only parameters required to monitor global performance and insure safety.

3.2 Design Constraints

Insofar as assembling the overall experimental flow train is concerned, the major constraint has been the geometric constraint imposed by the dimensions of the existing magnet bore. Figure 4 shows the available magnetic field distribution and bore dimensions for the existing Coal Fired Flow Facility (CFFF) magnet at UTSI. The magnet bore is 2.4 meters in length and has a rectangular cross-section. The magnet bore diverges in the horizontal plane (B field direction) from 23 cm at the entrance to 30.5 cm at the exit. The vertical bore dimension is constant at 40.6 cm.

The magnetic field distribution peaks at 3.2 Tesla and is relatively flat for only a distance approximately 1 to 1.5 meters. In order to maximize power density, which is proportional to the square of the field strength, it is desirable to have a uniform high strength field. A region approximately one (1) meter in length is shown in figure 4 which is suitable for the experiment. The generator must be able to fit within this volume. Maximum utilization of this volume would be afforded by a generator with a rectangular cross-section similar to the MHD generator channels previously tested in this magnet. On the other hand, rectangular channels are relatively expensive in comparison to cylindrical channels. In addition, high pressure combustors in general are universally constructed with a cylindrical geometry from considerations of structural integrity and thermal efficiency. Mating a cylindrical combustor to a rectangular channel requires a nozzle which, in the case of a supersonic exit velocity, accomplishes the cross-sectional shape transition upstream of the throat in the subsonic flow region. Such nozzles are costly and are difficult to fabricate. By selecting a circular geometry for the combustor and channel, a simplified system results. In this case, the cost for this simplicity is that the maximum outside diameter of the channel must be less than the smaller bore dimension or approximately nine (9) inches. The nominal

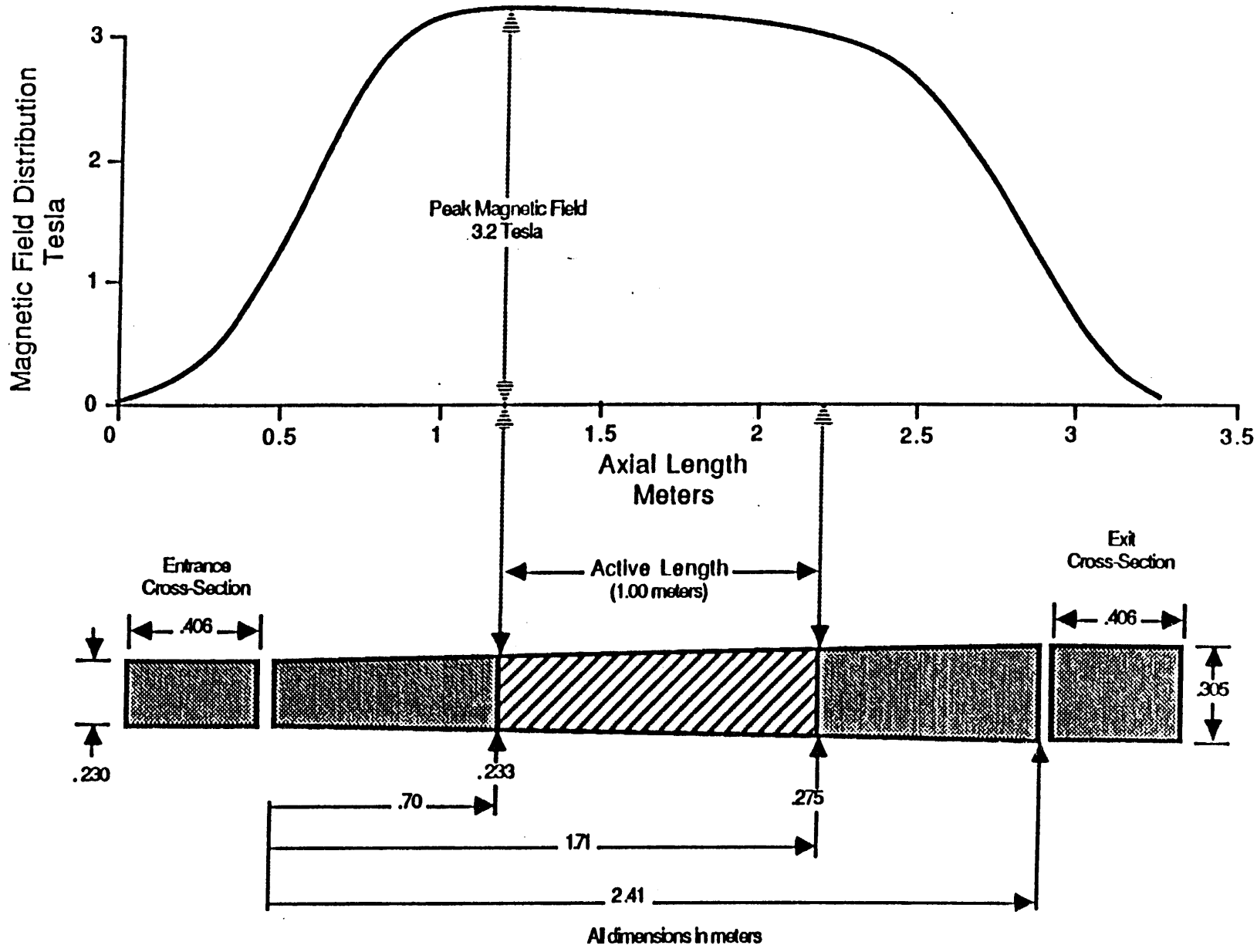

Figure 4. CFFF 3.2 Tesla Magnet Bore Volume and Magnetic Field Distribution.

outer diameter of the generator is taken to be eight (8) inches which permits a 1/2 inch thick glass laminate thermal shield to separate the channel from the magnet structure. The thermal shield is necessary to protect the magnet in the event of a plasma leak in the flow train either at a gasketed flange or a burn through elsewhere. After accounting for the component flange connection, pressure vessel wall thickness and internal heat shield thickness, the useable internal channel diameter is nominally taken to be three (3) inches.

To minimize thermal losses from the plasma, it is also desireable to have the combustor close coupled to the generator channel with a short nozzle. The same geometric constraints therefore apply to the portion of the combustor-nozzle combination which is located in the shielded region upstream of the useable active length depicted in figure 4. This region is within the magnet fringe field where the field ramps up from 0 to 3.2 Tesla. It should also be pointed out that the field distribution shown in figure 4 is the principal horizontal component. In the center of the magnet, the other field components are generally negligible in comparison with the horizontal component. In the fringe field regions, the field distribution becomes more three-dimensional, in that the vertical, horizontal, and axial components can be of the same order of magnitude.

The combustor and nozzle will therefore operate in a significant magnetic field strength environment. This is contrary to conventional design practice, since the MHD interaction will also be present in these components. That is, they will in essence be analogous to a short circuited MHD generator, and the plasma will have parasitic eddy currents induced in the fringe field. The effect of these eddy currents will be to impose a pressure drop and Joule heating on the plasma. In the combustor where the velocity is low, the losses are minimized in accordance with the power density discussions in section 2.0. However, since the nozzle is designed to produce an optimal power density

parameter at its exit, the losses should also peak here. Thus, these considerations provide an electrodynamic basis for the necessity of a short nozzle and close coupling the combustor to the generator as well. The only known precedent of a nozzle operating in a significant magnetic field is the Hercules C-MHD generator which was operated in the early 70's and produced one of the highest enthalpy extractions achieved.

From a volumetric and accessibility stand point, the geometric constraints of the magnet on the combustor are less than the channel. The magnet is an iron core saddle coil design. The geometry shown in figure 5 is appropriate for the bore within the iron pole pieces. Outside of the iron return frame, the saddle coil crossover limits vertical and horizontal accessibility as shown in figure 5. The coil force containment members restrict horizontal accessibility but not vertical accessibility. Beyond the force containment members, there is unlimited accessibility.

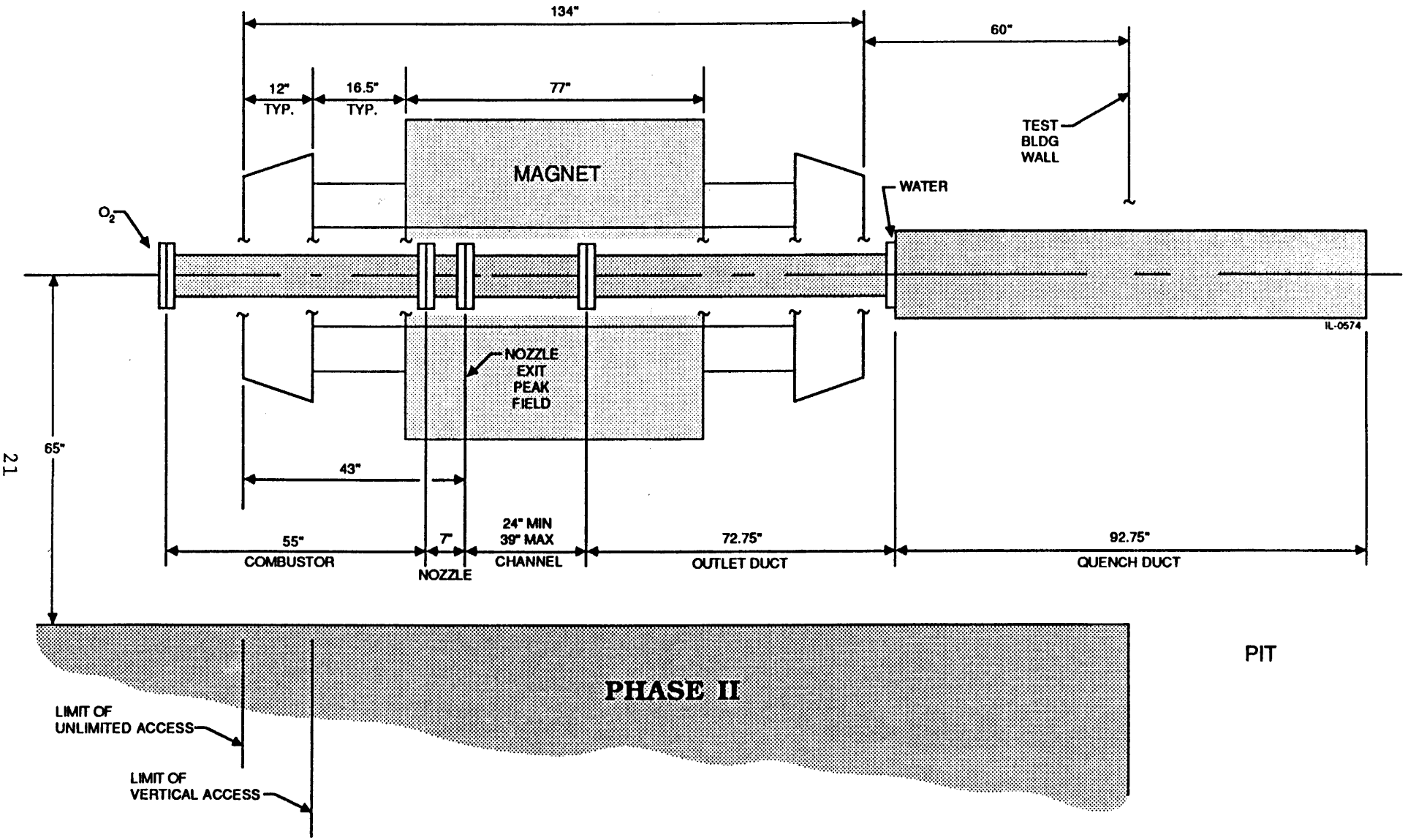

Figure 5. Sketch of Magnet with Flow Train Showing Accessibility of Combustor

3.3 Combustor Design

The nominal combustor design is shown in figure 6. The combustor is comprised of three metal pieces: the barrel, the injector face, and the nozzle. The barrel is an eight (8) inch diameter Type 304 stainless steel seamless tube having a 1/4 inch wall thickness and 54 inches in length. The injector end flange is welded exterior to the barrel while the downstream flange is interior to satisfy the magnet bore dimensional constraint. The combustor is to nominally operate at a combustion pressure of 600 psi and is supplied with gaseous oxygen of 1200 psi. The hoop stresses in the stainless steel barrel are 4500 and 9000 psi for these two pressures respectively. The ultimate tensile strength of the stainless steel is 89000 and 50000 psi at 100 and 1200°F respectively. The yield stresses for stainless are 28000 and 18000 psi for the same temperatures respectively. The steel barrel has at least a safety factor of two with regards to the hoop stress.

The fuel grain has a nominal outer diameter of six (6) inches and is encased in a laminated glass shell of 1/8 inch wall thickness. The encased fuel grain is in turn separated from the stainless steel barrel by a 1/2 inch thick insulator. As shown in the inset in figure 6, the internal shape of the fuel grain is that of a six spoked wagon wheel configuration with the inner and outer radial dimensions of the spokes being approximately 1 and 2-3/8 inches respectively. The fuel grain is of a uniform cross-sectional shape for most of its length. Near the nozzle end of the combustor, the outer grain spoke radius is reduced to 1-1/2 inches to mate with the nozzle contour. The fuel grain will be comprised of two half length sections which will nest (i.e. a lap joint) at their juncture for ease in shipping.

A pressure relief port is provided for in the combustor barrel as shown in figure 6. When installed in the magnet the pressure relief port will be positioned vertically between the coil force containment structures shown in

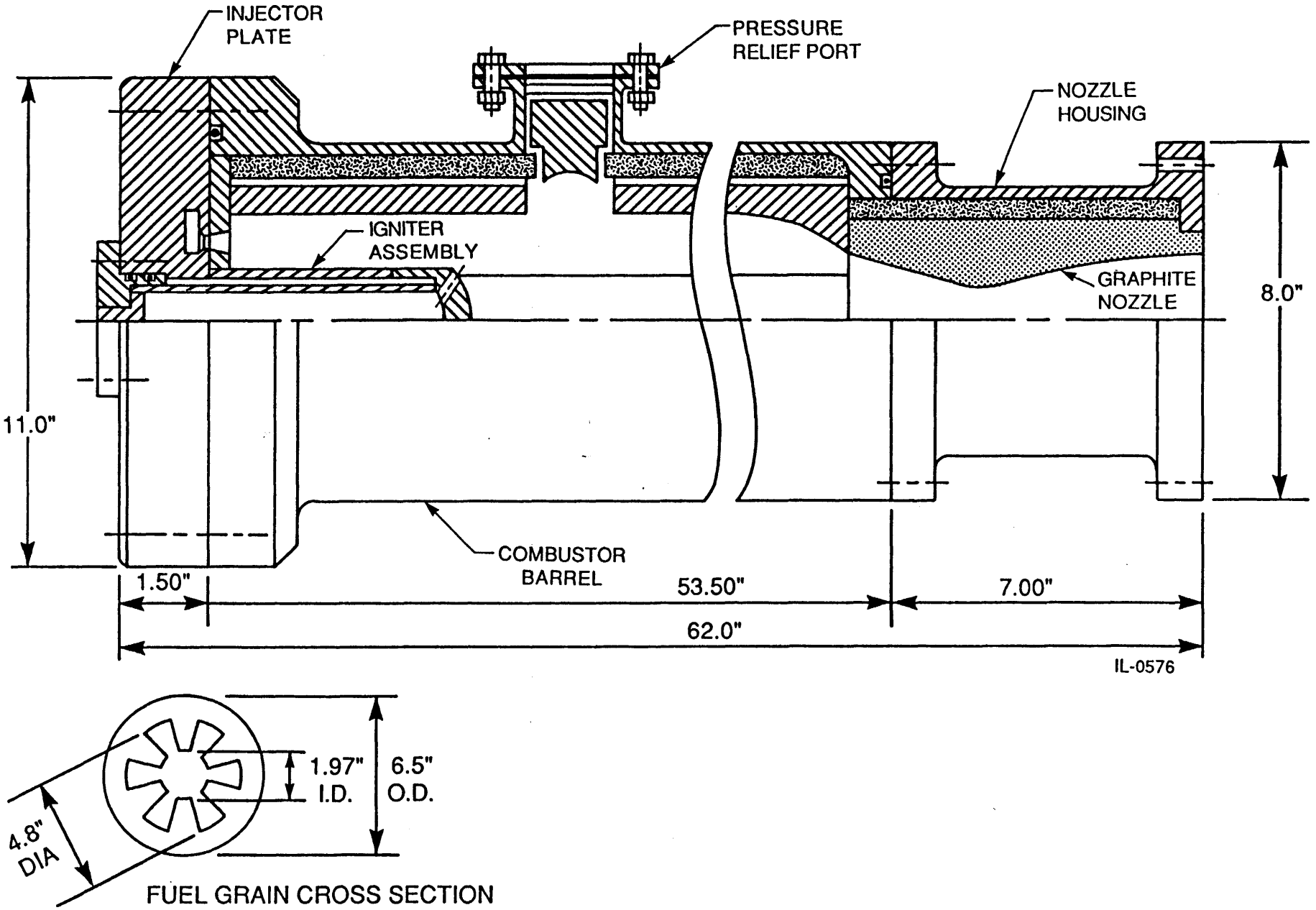

Figure 6. Preliminary Assembly Drawing of the Hybrid Combustor.

figure 5. The pressure relief port is comprised of a tube welded to the combustor barrel with an opening in the fuel grain to the central combustor cavity in the center of the fuel grain. The relief port is covered by a thin copper sheet behind which a 3/8 inch high steel shear piston is positioned. The shear piston carries an "O" ring seal. The steel shear piston in turn is positioned over a much higher insulating phenolic piston. In the event of an over pressure the shear piston will punch a circular blank from the copper sheet and the copper blank, shear piston, and phenolic piston would be expelled leaving an open port to the combustor's main cavity. The thickness of the copper shear disk determines the actual relief pressure and can therefore be controlled.

The injector is essentially in the form of a one (1) inch thick blind flange at the front of the combustor. In its center it has an opening for the igniter assembly and within its combustor side face an oxygen manifold is located. This manifold is constructed by milling a circular slot followed by welding a cover over it and drilling six injector holes in the cover. The manifold has a single outside supply connection which is not shown in the figure. The six injector holes are positioned to inject the oxygen along the fuel grain cavities between the spokes. A ceramic thermal insulator disk is positioned between the fuel grain and injector plate. The insulator plate is pinned to maintain its position so that it does not rotate and block the injector holes.

The igniter is comprised of a stainless steel pipe threaded into the injector plate. An insulating graphite sleeve on the outside is held in position by the graphite cap which is threaded onto the stainless steel pipe. The graphite cap has six (6) ports to direct the igniter combustion products to the six (6) interspoke cavities of the fuel grain. The interior of the igniter is shielded with a cylindrical phenolic liner. Finally, the outside

ignitor cap, which carries the "O" ring seals also contains a phenolic insulator for carrying leads for the electric match. In operation the ignitor chemicals are loaded in the ignitor along with an electrical wire glow element (electric match). The match ignites the chemical which provides the initial flame for starting the fuel grain. The igniter is reloadable without removal of injector plate. The preferred chemicals for the igniter are boron and potassium nitrate. However to achieve longer ignition times, a two (2) second maximum is desired, it may be necessary to use a different combination perhaps ammonium nitrate. The combustor vendor, REDEVCO, is currently testing the igniter assembly.

The aft end of the combustor is comprised of the nozzle closure which is simply a graphite nozzle surrounded by a ceramic insulator and encased in a double flanged stainless steel shell. The nozzle is replaceable since it is expected to erode significantly. The erosion may be both from thermochemical ablation and mechanical removal of material. The former is surface diffusion limited combustion of the graphite, much the same manner as the fuel grain burns. The difference between the nozzle graphite and the fuel grain is that the graphite is a much denser carbon matrix which is not held together with a thermally degradable binder. As a consequence, the fuel grain simply has a faster surface recession rate than the graphite in the nozzle. The condensed aluminum oxide species will mechanically erode the graphite in the nozzle through impact. This may prove to be the dominant material removal mechanism as is often noted in rocket and re-entry environments.

While not shown in the figure, the combustor will have one chamber pressure port and three thermocouples as part of its internal instrumentation. The combustor pressure port will be located in the injector plate. One thermocouple will be located on the back side of the fuel and two thermocouples will be located on the outer side of the graphite nozzle; one axially located

at the throat and one axially upstream of this location. During testing additional external thermocouples will be placed on the outer surface of the combustor barrel.

The thrust produced by the combustor will be borne by the injector head. The magnet bore constraints do not permit room or access for thrust containment within the bore. When installed in the magnet, the magnet's force containment members provide a suitable anchor point for containing the thrust. Thrust containment will be by a yoke which surrounds the enlarged flanges of the injector end. The yoke will be electrically insulated from the combustor to permit the combustor potential to float while the downstream end of the flow train is grounded.

Finally, a word on safety is necessary. For all practical purposes, the combustor has the outward appearance of that of a solid propellant rocket. This coupled with the knowledge that solid propellant rockets can and do explode and that an untried fuel is being tested has understandably caused safety concerns. There is an important difference between the combustor and a solid propellant rocket in that the fuel in a rocket contains its own oxidizer. Therefore, solid propellant fuel will burn in a confined space and its burning rate will exponentially increase with the confining pressure. Solid propellant rocket fuels can detonate. In the present experimental combustor there will be no oxidizer in the fuel. It is not expected to have a severe burning rate dependence with chamber pressure, and it cannot detonate. Combustor over pressures will tend to cut off the oxygen supply. However, the grain, the igniter, and nozzle are all subject to breakage, such that it could be envisioned that the nozzle could become blocked. The relief port is incorporated in the combustor primarily for such an eventuality.

3.4 Nozzle Design

As pointed out previously the nozzle will be subject to severe erosion and is anticipated to be the weakest link in the flow train. On the one hand, the nozzle length should be short to close couple the combustor to the generator and minimize thermal and electrodynamic losses. On the other hand, the throat region which will be exposed to the most severe thermochemical and erosive environment should have as large of a radius of curvature as possible for its length in order to maximize its durability in this environment. The nozzle is designed to expand the plasma from the combustor conditions to a Mach number of 2.5 at its exit. The area ratio for this expansion is approximately 4.0 and for a specified exit diameter of 3.0 inches, the throat diameter required is approximately 1.5 inches (figure 2).

Downstream of the throat the plasma flow is accelerating supersonically. The nozzle contour in this region must be aerodynamically contoured to avoid oblique shock formation or flow separation. The transition from the nozzle exit to the generator entrance should be smooth with no misalignment steps or angular discontinuities.

The preliminary nozzle design is shown in figure 6. The nozzle is eight (8) inches in overall length with the subsonic portion to the throat being 3.0 inches in length. The 5.0 inch length supersonic region downstream of the throat has been contoured in accordance with inviscid method of characteristic calculations. The contour schedule for the nozzle internal loft is given in Table I. In the table, which has been abbreviated from the full computation, the uneven axial position increments are a result of the selection of the nearest actual computed points.

Table I. Nominal Nozzle Internal Loft

Axial Position, x Inches	Radial Position, y Inches	Area Inches^2	Wall Angle Degrees
0.00	1.50	7.06	-26.2
0.50	1.27	5.07	-23.0
1.00	1.08	3.68	-18.8
1.50	0.94	2.76	-14.5
2.00	0.83	2.18	- 9.9
2.50	0.77	1.86	- 5.2
3.00	0.75	1.76	0.0
3.48	0.82	2.10	18.6
4.08	0.99	3.06	31.7
4.52	1.10	3.81	26.7
4.99	1.20	4.57	22.8
5.54	1.31	5.37	18.1
6.03	1.38	5.96	14.2
6.55	1.43	6.45	10.2
7.00	1.47	6.77	7.9
7.48	1.49	6.98	3.7
8.00	1.50	7.07	0.0

Additional calculations which include viscous effects were performed for the nominal axisymmetric nozzle shape using the VNAP program developed by Cline[5]. These calculations, shown in Figure 7, give the velocity and Mach number profiles and boundary layer development along the nozzle length for the nominal design loft. In addition, the possibility of shortening the overall nozzle length was explored and results for a 6-1/2 inch nozzle are shown in figure 8. The 6-1/2 inch nozzle has a 1/2 inch shorter subsonic section and a one inch shorter supersonic portion. These calculations indicate that no separation occurs in the shorter candidate nozzle, and this design would be a viable alternative, if necessary, for the generator testing. The simplicity of the nozzle design shown in figure 6 lends itself to shortening rather easily. In fact, the base cost of the overall nozzle is sufficiently low for this simple design and a shorter nozzle would not be a difficulty.

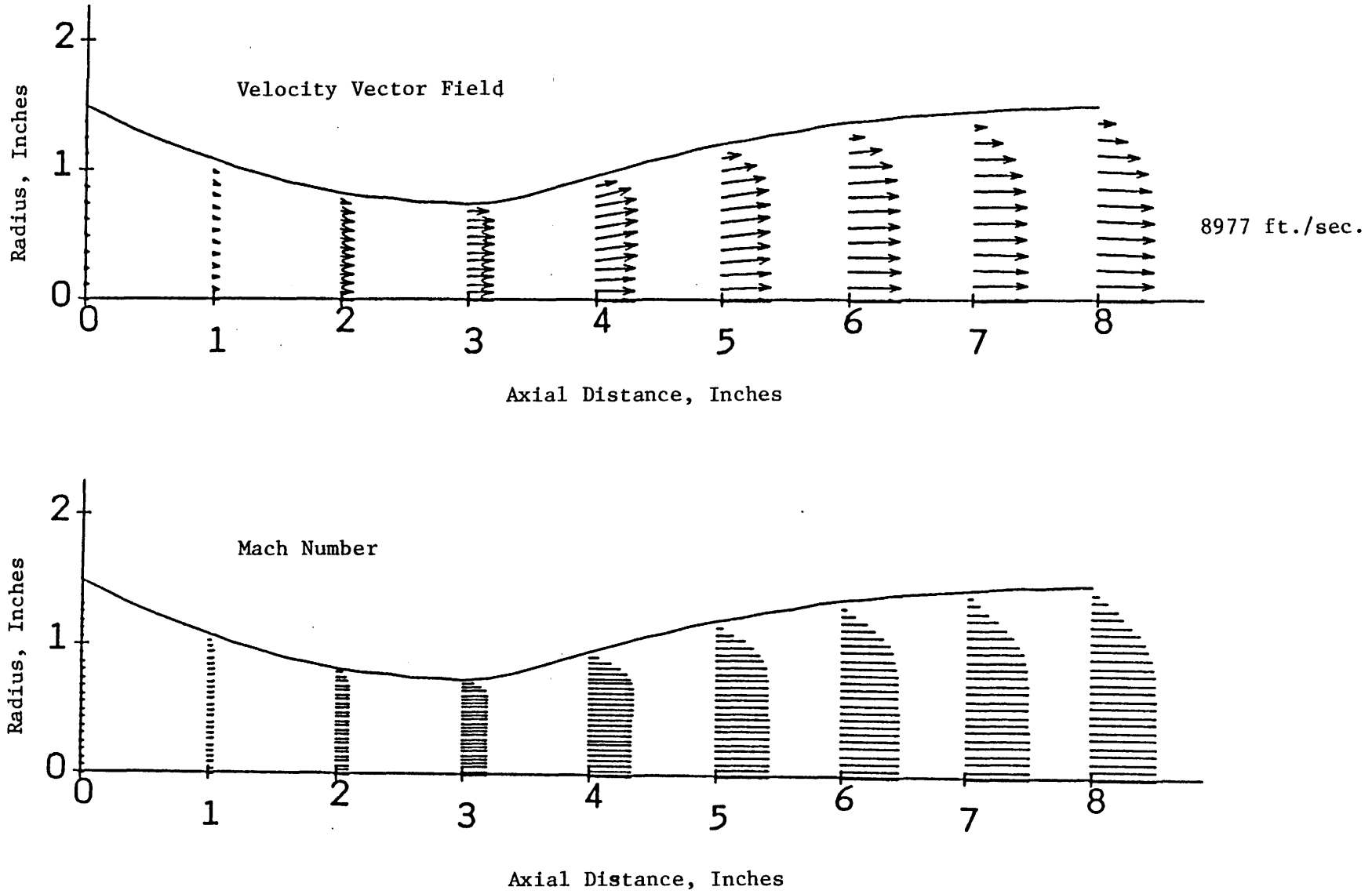

Figure 7. Calculated Velocity and Mach Number Profiles for the Nominal Eight (8) Inch Long Nozzle Contour.

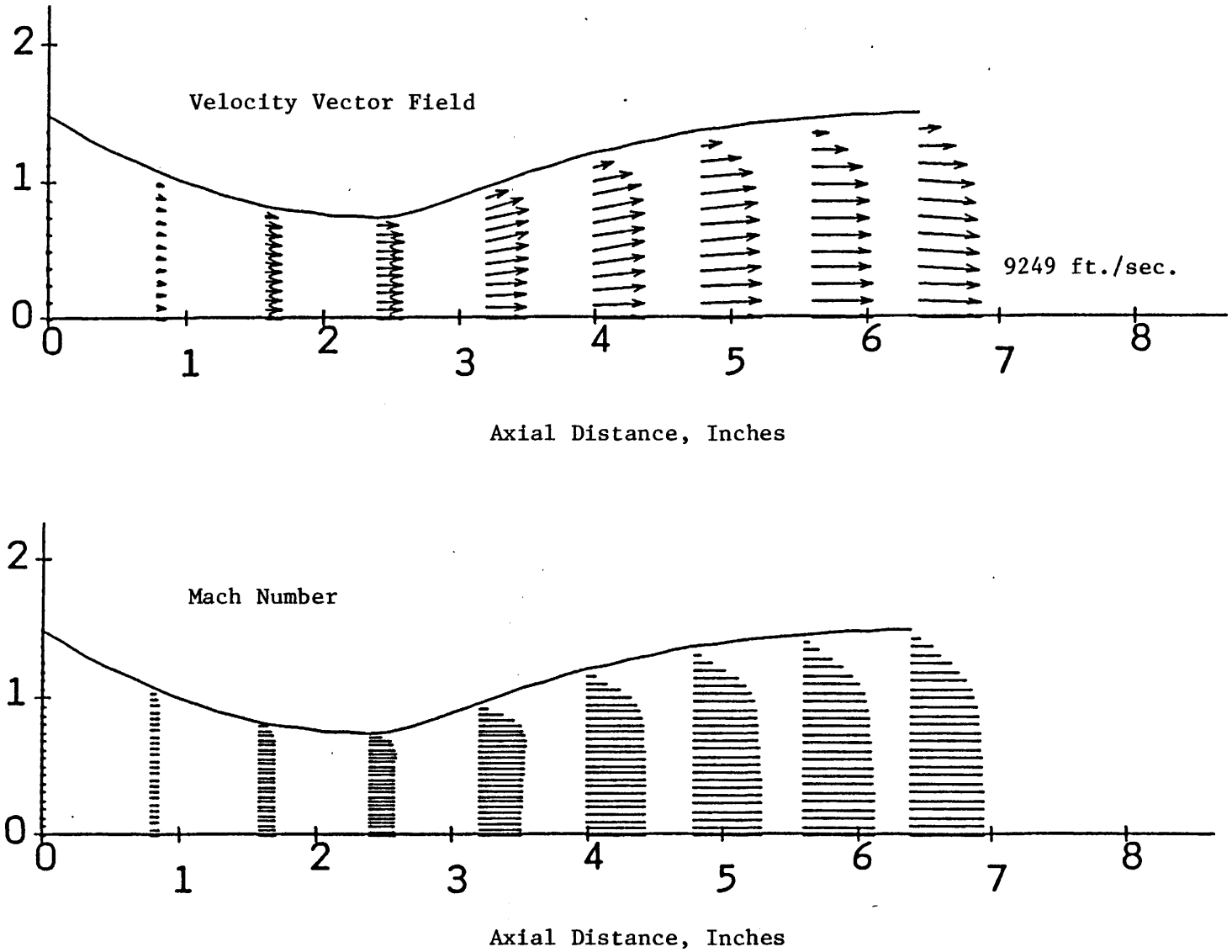

Figure 8. Calculated Velocity and Mach Number Profiles for a Shortened Nozzle Design.

3.5 Generator Performance

Detailed parameter studies of generator performance were performed as a significant part of experiment design and were reported fully in the semi-annual report[3]. These studies considered parametric variations of combustor pressure, inlet Mach number, and electrode diagonalization angle. A summary of the findings of these parametric studies were:

1. Combustion pressure strongly influences generator length which increases with increasing combustor pressure. The mean level of power density achievable for a given generator design is only mildly sensitive to the combustor pressure. This is shown in figure 9. However, the MHD interaction is a strong function of the combustor pressure and it is for this reason that generator length increases with increasing pressure.
2. The generator inlet Mach number has a strong influence upon the power density level that can be achieved as indicated in the nozzle design discussion.
3. In a two terminal diagonal conducting wall configuration (DCW) optimal performance is obtained for shallow wall angles on the order of 30°.

Based on these studies the nominal operating point is selected to be that of a combustor pressure of 40 atmospheres and a channel inlet Mach number of 2.5. Other conditions of interest are summarized in Table II for the nominal operating point.

The generator design performance calculations are summarized in Table III and figures 10 and 11. Table III indicates that the nominal power prediction is 1.8 megawatts with a power density of 600 MW/m^3. In figure 10 the calculated plasmadynamic and electrodynamic parameters are presented as axial distributions for four levels of load current. The plasmadynamic characteris-

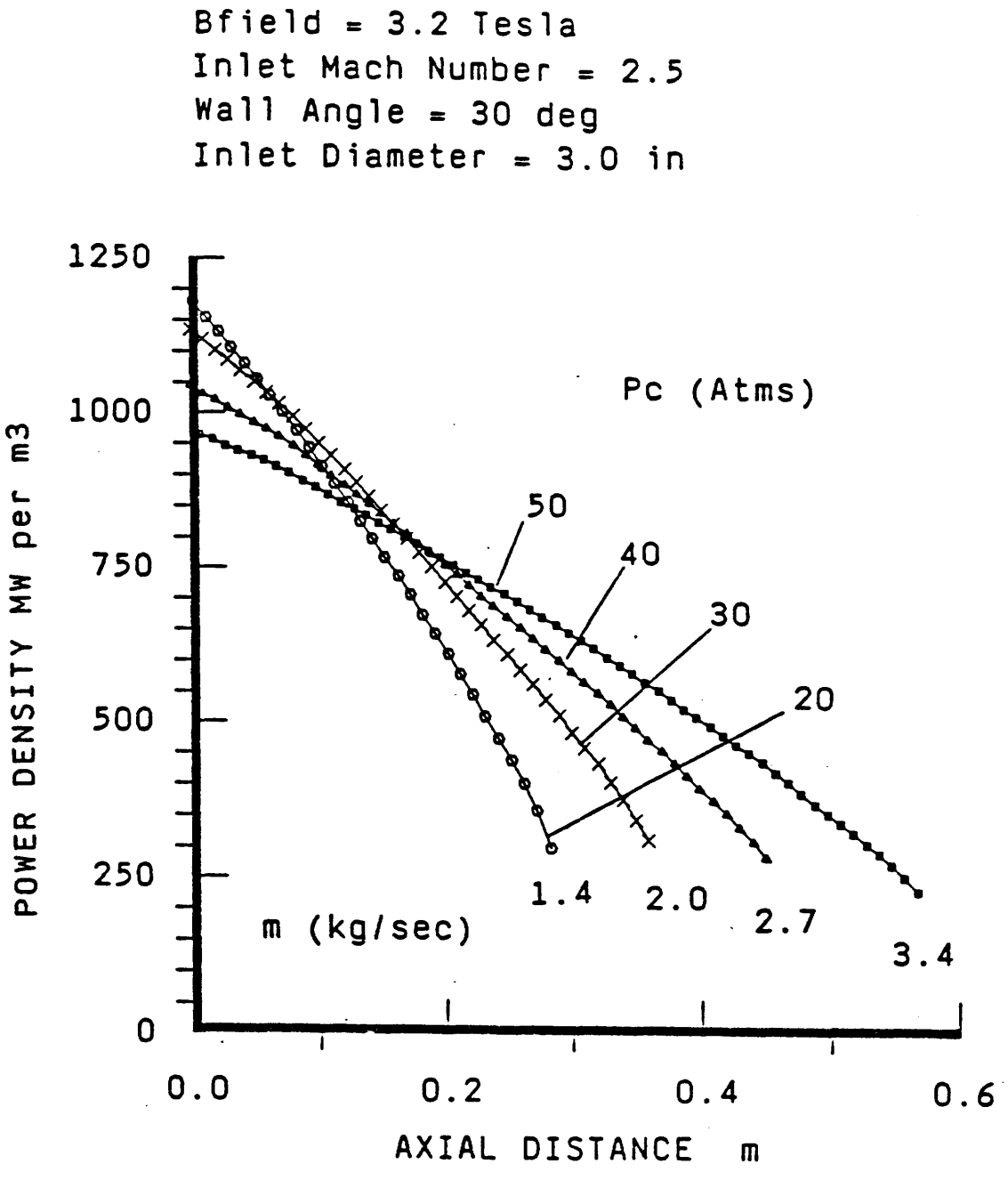

Figure 9. Effect of Generator Interaction with Operating Point - Power Density, Mass Flow and Supersonic Generator Length.

TABLE II. MHD GENERATOR DESIGN FEATURES AND OPERATING POINT

Combustion:	Fuel	Al:C (50:50)
	Oxidizer	O_2 (gas)
	Stoichiometry	0.77
Mass Flow Rate		2.8 kg/sec
Combustion Pressure		40 Atms
Combustor/Nozzle Heat Loss		2% Q_t Input
Nozzle Throat Diameter		0.039 m
Nozzle Exit Diameter		0.076 m
Nozzle Area Expansion (A/A*)		3.80
Nozzle Length		0.20 m
Generator Length		0.46 m
Generator Wall Divergence		2.03°
Generator Mean L/D		5.1
Diagonalization Angle		30°
Peak Magnetic Field		3.2 Tesla
Generator Inlet Mach Number		2.5
Generator Inlet Pressure		2.15 Atms
Generator Inlet Temperature		3246 K
Generator Inlet Conductivity		104 S/m
Generator Inlet Velocity		2478 m/sec

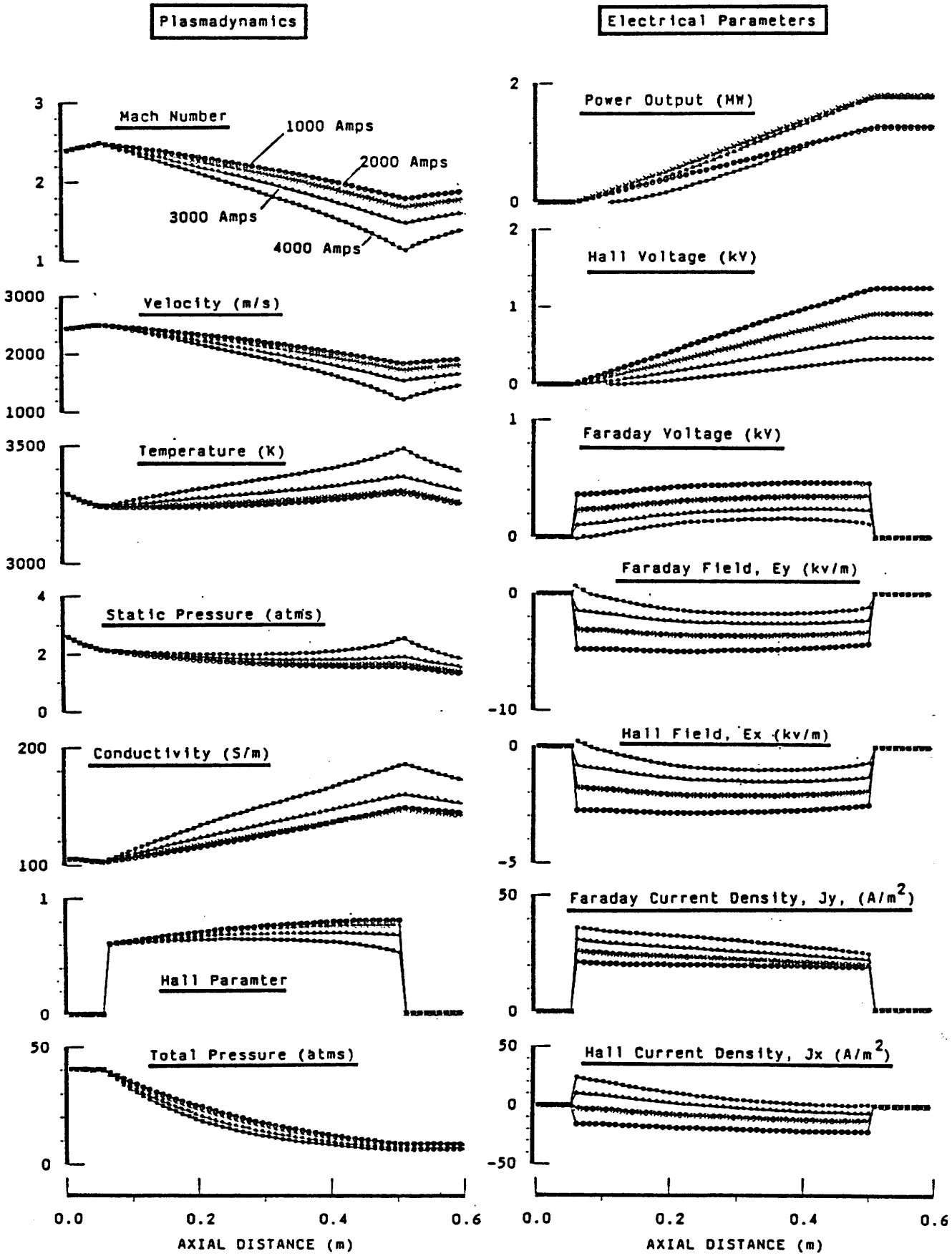

Figure 10. Calculated Plasma and Electrical Parameter Distribution for the Nominal 30° DCW Generator Channel.

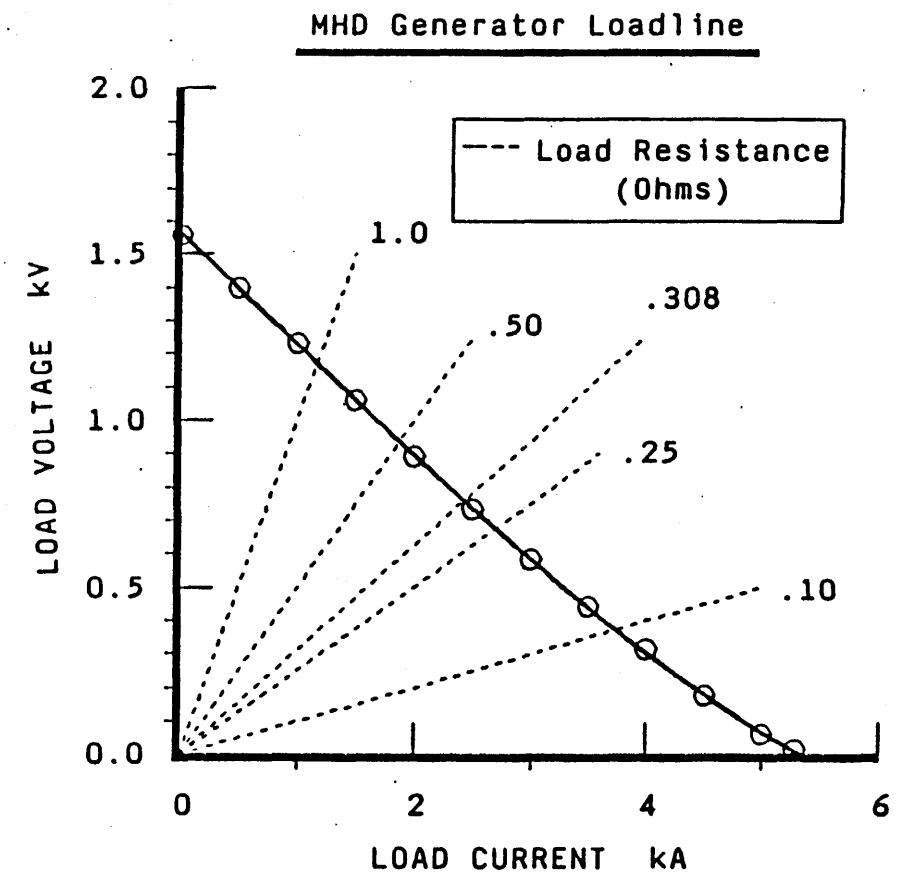

a) Load Line

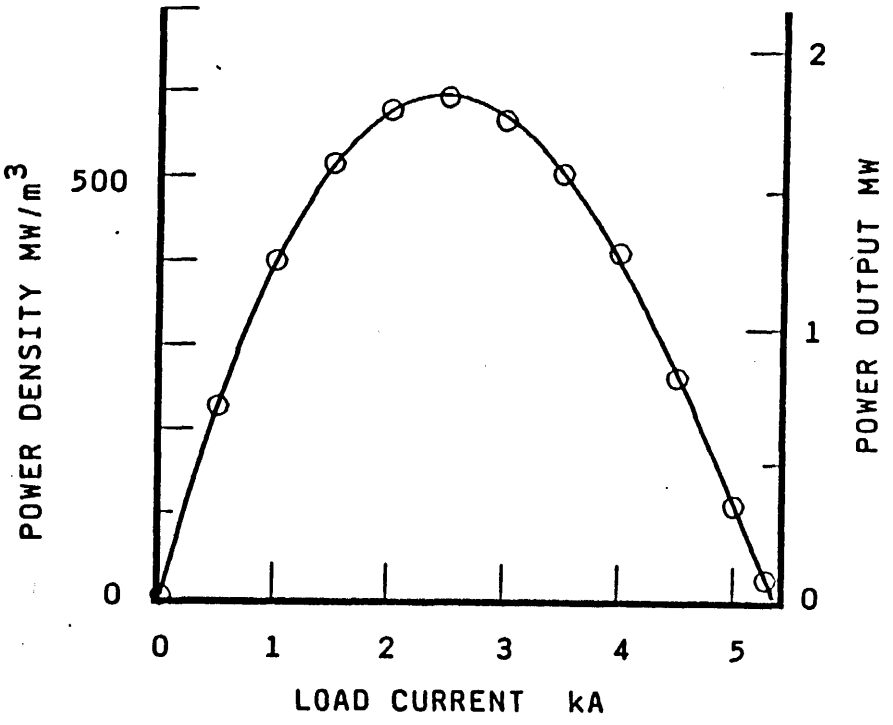

b) Power Characteristics

Figure 11. Calculated Load and Power Characteristics for the Nominal 30° Wall Angle DCW Generator Channel.

TABLE III. THEORETICAL MHD GENERATOR PERFORMANCE
(Maximum Power Operation)

Total Mass Flow Rate	2.8 kg/sec
Thermal Input	9.704 MW
Combustion Pressure	40 Atms
Combustion Temperature	4318 K
Generator Length	0.457 m
Generator Mean Flow Area	58.6 cm^2
Generator Volume	3076.9 cm^3
Diagonalization Angle	30°
Internal Surface Area	0.23 m^2
Average Heat Flux	380 Wts/cm^2
Load Current	2440 Amps
Load Voltage	751 Volts
MHD Power	1.83 MW
Specific Power Output	0.66 MJ/kg
Interaction Parameter (Ip)*	0.99
Power Density	600.6 Mw/m^3
Enthalpy Extraction	19.0%
Generator Efficiency	78.6%
Electrical Efficiency	38.6%
Mean Static Pressure	3.1 Atm
Mean Static Temperature	3219 K
Mean Velocity	2101 m/sec
Mean Mach Number	1.90
Mean Conductivity	127 Mho/m
Mean Hall Parameter	0.7
Open Circuit Voltage	1574 Volts
Short Circuit Current	5350 Amps
Internal Impedance	0.31 Ohms
Joule Heat Dissipation	1.48 MW
MHD Push Power	-4.79 MW

*MHD Interaction Parameter Based Upon Pressure, $I_p = \int_0^x \frac{\bar{J}\times\bar{B}}{p}\,dx$

tics are typically indicative of a decelerating flow in which the deceleration is proportional to the load current. That is, the velocity, Mach number, and total pressures decrease faster as the load current increases while the temperature, static pressure, and conductivity behave oppositely. For a load current of 4 K amps the plasma flow approaches a choking condition at the channel exit. For all load currents the static pressure at the channel exit is greater than atmospheric, and the total pressure is in excess of five atmospheres. Diffusion and pressure recovery will not be required to prevent flow separations in the generator.

The loadline and power characteristics at the nominal generator design case are shown in figure 11. The loadline is nearly linear throughout most of its extent with a shallow slope indicative of the generator low conductivity. The loadline is not straight, but rather curvature is evidenced at the terminal ends. At the open circuit end, the reduced Joule heating is less effective in offsetting the temperature and conductivity reductions accompanying the plasma expansion. The loadline slope and internal generator impedance are as a consequence slightly increased. At the short circuit condition the opposite situation occurs. Lines of constant load resistance are superimposed on the loadline for reference. Comparing the loadline plot with the power plot in figure 11 an optimal load resistance of approximately 1/3 ohm will be required.

The generator loft is that of a conical frustum have a three (3) inch diameter inlet and a 2.3° conical expansion angle in accordance with the magnet dimensional constants previously discussed in section 3.2. Mechanical design of the generators has been deferred until completion of the combustor tests. In their mechanical design, however, they will be similar to the combustor. The generators will be comprised of an outer pressure vessel of

either steel, electrically insulated from the inner electrodes or laminated glass with flanges at either end. Laminated glass is the preferred material on the basis of electrical insulation. The inside will be comprised of graphite electrode elements separated from the pressure vessel with a ceramic electrical and thermal insulator similar to the fuel grain arrangement in the combustor as shown in figure 6.

4.0 COMBUSTOR TESTING

All testing in conjunction with the experiments to be performed in the program will be conducted in Bay 2 of the Department of Energy (DOE) Coal Fired Flow Facility (CFFF) at the University of Tennessee Space Institute (UTSI). A floor plan of the CFFF is shown in figure 12. As shown in the figure the CFFF has three test bays. Test bay #1 is currently occupied by a coal fired MHD flow train which is utilized on a continuing basis under an ongoing DOE research program. Test bay #2 is the logical choice for both combustor and generator tests of the present program due to its proximity to the magnet utility terminations as well as its accessibility to the outside with an overhead door. Bays 2 and 3 are unoccupied and their availability is premised under the usage that they cannot interfere with the ongoing activities use of bay 1.

Combustor testing at the CFFF was scheduled to be completed during the first year of the program. However, slippage in the schedule has precluded the completion of these tests between August and mid-November when no testing was scheduled in bay 1. With the expected arrival of the combustor in early November, a test window extending from latter November to April will be available for conducting the current program combustion testing.

When the combustor and generator are eventually installed in the magnet, downstream ducting will be required for conveying the exhaust outside of the facility. This ducting must meet the same magnet bore geometric constraints as the combustor and generator. The ducting, shown in figure 13 will be comprised of two sections. The first section is a simple, refractory lined extension of the generator channel to the downstream exit of the magnet bore. The second section is of similar construction, but includes a water quench for the exhaust gasses. The quench is included to cool the exhaust as it is

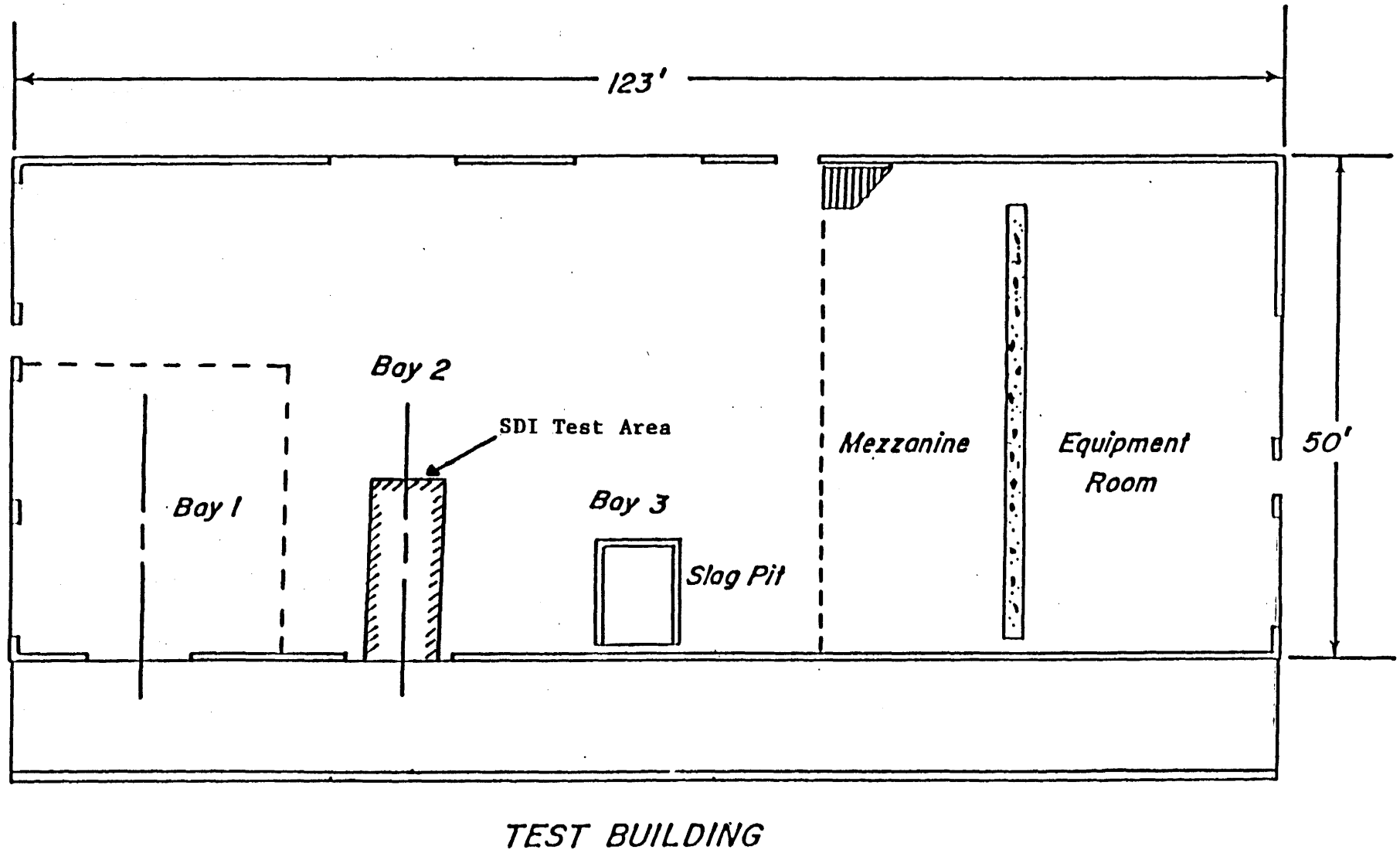

Figure 12. Floor Plan of Test Building Showing Location of Combustor Test Area

dumped outside of the building. Exterior to the building there is a 30-40 foot horizontally clear area beyond which the downstream pollution control equipment associated with the bay 1 flow train is located. The water quench is intended as a protective measure for this equipment.

In testing the combustor alone, the combustor and exhaust ducting will be mounted directly to the floor of the test area as shown in the sketch in figure 13. The thrust, which is estimated to be between 2000 and 3000 pounds will be borne by the forward combustor attachment. The other various saddle attachments will be used to secure the test train to the floor.

Bay 1 has an overhead mezzanine containing the magnet power buss ducting as well as various other instrumentation. Also, the ceiling of the test building contains routings for the various utilities in the building including water, fuel oil, gases, and electricity. Therefore as a possible damage control measure, a shield will be placed around the combustor during the initial testing. The shield will be comprised of a 1/2 inch thick, 5 ft. diameter steel half cylinder. While a catastrophic explosion is deemed extremely remote, the proper operation of the combustor blowout port must be accounted for and this is the primary purpose of the shield.

4.1 Oxygen System

While the CFFF facility has a large capacity of gaseous nitrogen, oxygen, and compressed air supplies as part of its utility complement, the supply pressures are insufficient for satisfying the requirement of the present program other than for purge and calibration requirements. In addition the air systems (particularly the high pressure air system) are not oil free and therefore cannot be used to calibrate the oxygen system.

A separate high pressure gaseous oxygen system is required for the combustor testing. The oxygen supply will be from a manifolded group of "K" bottles as shown in figure 14. These bottles are nominally charged to 2000

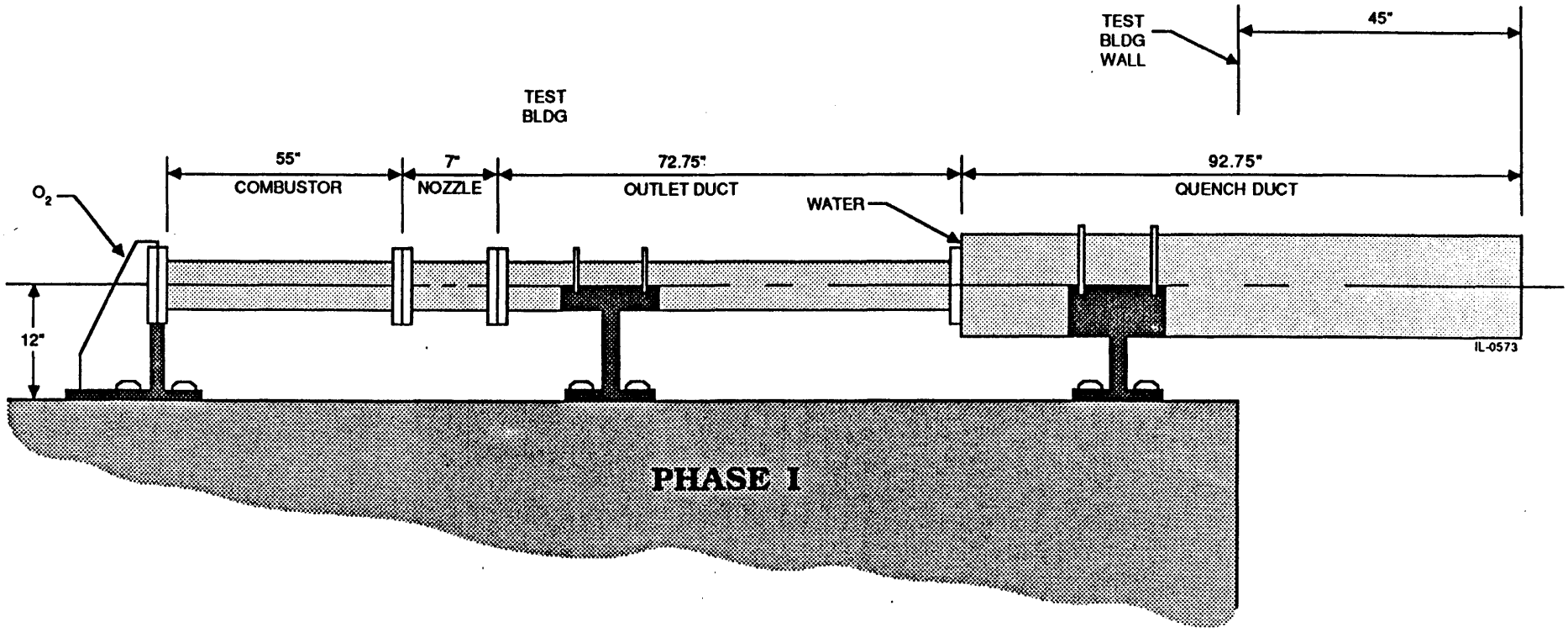

Figure 13. Sketch of Flow Train System for Testing of the Combustor in Bay 2 of the CFFF Facility

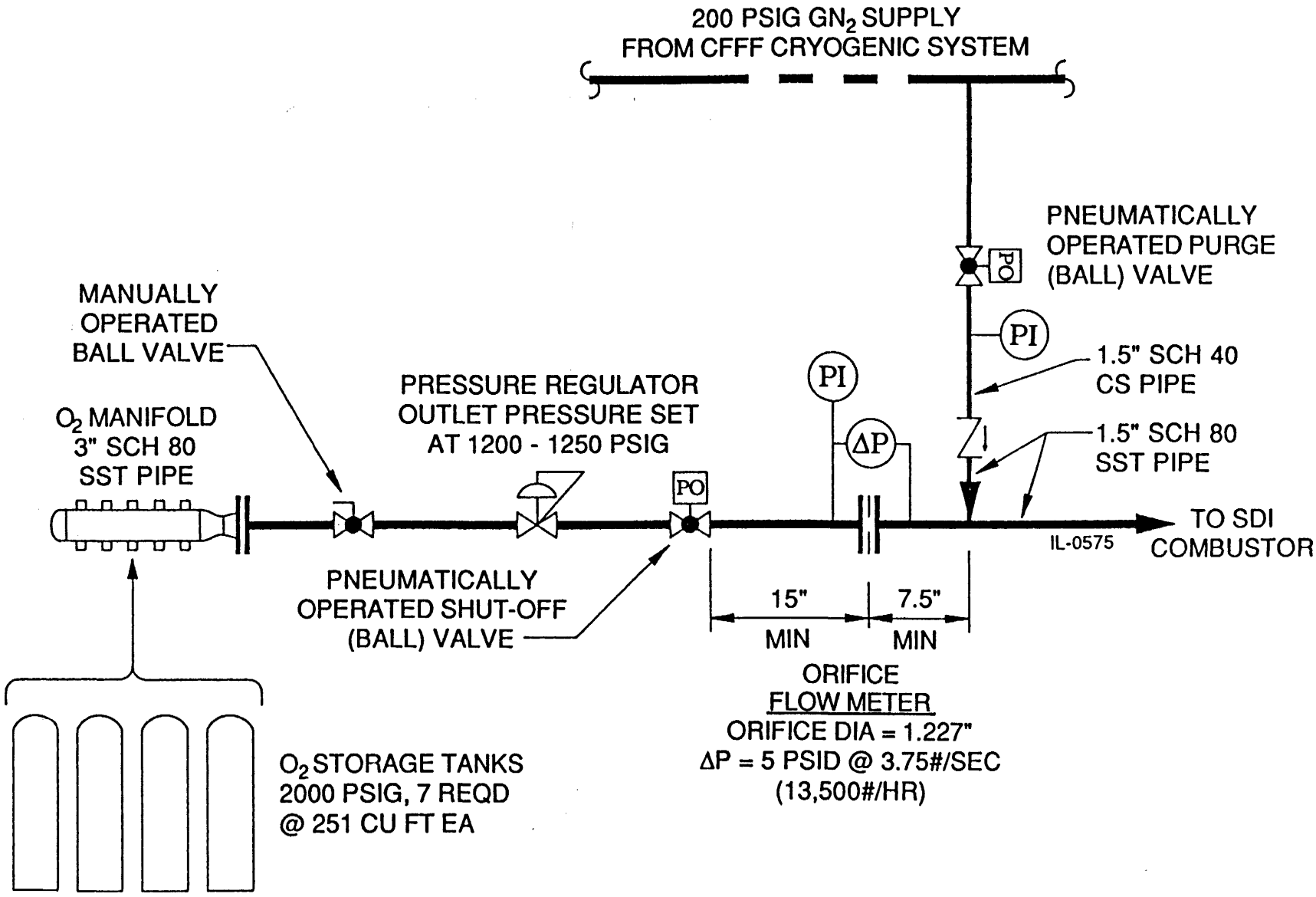

Figure 14. Schematic of the Gaseous Oxygen System for Combustor and Generator Testing in the CFFF Facility

psi and contain 250 scf or approximately 21 pounds of gas. The combustor supply pressure is required to be approximately 1200 psi to maintain choked injection orifices at the design combustion pressure of 600 psi. Therefore, the bottles are only useable down to a pressure of 1200 psi, or equivalently, 8.4 lbs of oxygen is available from each fresh bottle. The oxygen consumption rate for the combustor is 3.74 #/sec which will require a minimum of 56 lbs O_2 for a combustor fuel load of 15 seconds duration. Therefore a minimum of seven (7) bottles will be manifolded together to comprise the supply.

The piping schematic in figure 14 shows various valves and controls for the oxygen system. A manual line valve along with manual valves on each of the bottles are used to change out individual bottles at the manifold and to isolate the downstream line when necessary. The pressure regulator and shut-off valve, shown as separate functional units in the figure, are in fact in a single control valve of a fail closed design. That is, the valve is pneumatically opened against a spring such that loss of electrical control of actuating air the spring will mechanically close it.

Nitrogen purge is tied to the oxygen supply with a pneumatically operated valve. Since the oxygen pressure is substantially higher than the available nitrogen pressure, a check valve is used to prevent back flow into the nitrogen supply. The check valve also provides for an automatic start of purge nitrogen at the end of the combustor operation. When the oxygen valve closes, the pressure in the line to the combustor will fall. Assuming that the nitrogen valve is open, as soon as the oxygen pressure in the line drops below the nitrogen supply pressure, the check valve will open and the oxygen line and combustor will be purged. Purge flow rate will be approximately 1/6 the oxygen flow rate or approximately 0.6 lbm/sec. An orifice in the oxygen supply line will be used to monitor oxidizer flow rate during the operation.

As a cross-check, the bottle pressures before and after a combustor firing will be used to determine the total flow and mean flow rate as well.

For powered generator operation, an insulating section of high pressure hose will be used to connect the oxygen supply to the combustor. This will permit the combustor potential to float while the oxygen supply remains at ground potential. This insulation is not required nor will be used for the combustor testing.

4.2 Test Program

The test program for the combustor will be done in three steps: oxygen system calibration, igniter testing, and the combustor testing. Each of these are considered separately in the following.

1. Oxygen System Calibration

After the facility modifications for the oxygen system are installed, the system will be calibrated with nitrogen. Available facility nitrogen will be used to check the operation of the control valve and control orifice pressure drop. The combustor will be used as a downstream load for the system. The low pressure calibration of the control orifice will be checked against facility flow measurements for accuracy. Extrapolation of the data to higher pressures with account for the molecular weight difference between nitrogen and oxygen will be made for a preliminary check of the proper orifice size.

With satisfactory completion of the preliminary system check out, high pressure gaseous nitrogen in "K" bottles will be used to verify the high pressure operation of the system. Short flow bursts of less than five (5) seconds duration will be used to check the system and measure the mass flow using the low pressure orifice calibration data extrapolated to higher pressure and mass flow rates.

The nitrogen bottle supply pressure will be recorded before and after each test. The supply pressure drop test duration and volume of the supply will provide an independent check for the validity of the extrapolated low pressure mass flow calibration.

2. Igniter Tests

Two igniter tests are necessary. The first igniter test will be comprised of the igniter alone. That is, the combustor head and igniter without the remainder of the flow train and the igniter exposed to free air. This test will be a shakedown test to verify controlled ignition and time the duration. No significant data will be taken but rather the igniter flame characteristics will be visually observed.

For the second igniter test, the flow train will be used intact, but nitrogen will be supplied to the oxygen system. The flow train will be purged with low pressure facility nitrogen initially which will then be operated using a visual cue (camera and mirror) to verify ignition. When ignition is verified, the main oxygen system control valve will be opened allowing the high pressure nitrogen to enter the combustor. The visual cue will again be used to determine whether the igniter flames out. Combustor pressure will be monitored during this test as a diagnostic.

The purpose of the second test is to insure that the igniter does not flame out before the main oxygen arrives at the combustor. During combustor start-up it is assumed that inert nitrogen will be in the combustor and in the oxygen supply line downstream of the oxygen control valve. The upstream line from the control valve is assumed to be initially charged with oxygen. Thus, it can be assumed that for a short period after the control valve is opened an inert

gas will flow through the combustor and the igniter must be able to sustain this transient. Transient data will be taken on combustor chamber pressure and oxygen line pressures to determine the proper time sequencing between igniter and oxygen line control valve opening.

3. Combustor Tests

The combustion tests will be performed in the same manner as the previously described igniter test with the exception that oxygen will be used in the main oxidizer system. The tests will be preprogrammed in duration and more reliance on the facility control system will be required. Combustor pressure cues, if possible, will be incorporated as a confirmation of igniter operation before committing to oxygen supply opening. Combustion chamber pressure will be the primary on-line diagnostic measurement.

Data taken during the run will be comprised of the combustion chamber pressure, combustor thermocouple temperatures, oxygen orifice plate pressures (O_2 mass flow) as functions of time. In addition, the manifolded oxygen supply pressure and combustor barrel section weight will be recorded before and after a run. The combustor consists of three parts; the head, the barrel, and the nozzle. The fuel load is cast in the barrel section. The fuel consumption desired is approximately 1.15 kg/sec of run time. Therefore, weighting will be used to determine the fuel loss which in turn will be used to verify the burning rate, total flow rate, and combustion stoichiometry.

It is anticipated that three (3) to five (5) runs can be achieved with a single fuel load. Initially the runs will be limited to three (3) seconds to verify repeatability, and the thermal soak

characteristics of the design. Three (3) thermocouples on the back side of graphite nozzle insert will be monitored for the thermal soak characteristics. Data taking on the thermocouples will proceed for a time of at least thirty (30) seconds after oxygen shut-off. One five (5) second run with the initial fuel load shall be made to provide a good average for the stoichiometric data.

With depletion of the first fuel load, a second fuel load will be tested. The second fuel load may have compositional changes such as particle size or binder content depending on the results obtained from the analysis of the data for the first firings. The second fuel load will be tested in the same fashion but with fewer runs of longer duration.

During the combustion testing the nozzle dimensional characteristics will be recorded to determine the erosion rate of the graphite. A second nozzle will be available for replacement with the fuel reload if necessary.

Oxygen system adjustments between tests will be comprised of supply pressure changes or orifice size changes. It would be expected that the latter would be for a coarse change while the former would be more appropriate for finer changes.

5.0 PROGRAM SUMMARY

In the following the seven tasks for the program are summarized and discussed.

Task 1. Analysis

During the first year analytic studies for the optimal fuel composition, channel lofting and combustor testing were completed. Data analysis of the combustor testing was not possible with the delay in testing. Test planning and generator data analysis are the second year function.

Task 2. Mechanical Design

Detail design of flow train components required for the combustor tests was completed during the first year. Detailed design of the magnet bore liner, thrust support, and generator channels are deferred until the second year. Specifications for the competitive procurement of the combustor were completed.

Task 3. Component Procurement

During the first year REDEVCO was awarded a contract to supply the complete combustor with an additional nozzle, fuel load, and ignitor system. Delivery of the combustor is anticipated in early November. Procurement of all materials for performance of the combustor task was completed. Fabrication of the exhaust ducting and support saddles was not completed. During the second year materials for the generator testing will be procured, and the magnet associated flow train support stands will be completed.

Task 4. Facility Modifications

The oxygen supply was designed and the procurement of materials for its implementation initiated. No installation was performed. Installation will be initiated after current Bay 1 testing in the CFFF is completed in mid-November. Second year efforts are related to generator

testing and will involve primarily magnet utilities and load bank installation.

Task 5. Combustor Test

Combustor tests scheduled for the first year were not completed. It is expected that these test will be completed by February 1, 1989.

Task 6. Generator Test

No effort was scheduled during the first year as this is in its entirety a second year function.

Task 7. Management

All periodic reporting requirements scheduled for the first year were completed. This task will continue throughout the second year.

In summary, all objectives except the conductance of the combustor tests were completed during the first year. The delay has not caused any financial burden and the program is still within its projected costs. It is expected that with the completion of the combustor tests during the first quarter of the second year, the program will meet its planned conclusion with generator testing completed during the second year of the two-year effort.

6.0 REFERENCES

1. Aleshin, M.H., et al, "Generator of Plasma on the Powder-Like Fuel of the Pulse Geophysical Installation," Proceedings of the 8th International Conference on MHD Electrical Power Generation, Moscow, 1983.

2. Volkov, Y.M., et al, "Investigation of Electrophysical Characteristics of the Combustion Products of the Metallized Powder-Like Carbon Fuels," Proceedings of the 8th International Conference on MHD Electrical Power Generation, Moscow, 1983.

3. Lineberry, J.T., Schmidt, H.J., Chapman, J.N., "Semi-Annual Report for An Innovative Demonstration of High Power Density in a Compact MHD Generator," University of Tennessee Space Institute, May 1988.

4. Crawford, L.W. and Lineberry, J.T., "Factors Affecting MHD Power Generation Using Powdered Aluminized Fuels," AIAA-86-1066, 4th Fluid Mechanics, Plasmadynamics Conference, Atlanta, GA, May 1986.

5. Cline, Michael C., "VNAP2: A Computer Program for Computation of Two-Dimensional, Time-Dependent, Compressible, Turbulent Flow," Los Alamos National Laboratory Report LA-8872, August 9, 1981.